Since January 2020 Elsevier has created a COVID-19 resource centre with free information in English and Mandarin on the novel coronavirus COVID-19. The COVID-19 resource centre is hosted on Elsevier Connect, the company's public news and information website.

Talanta 252 (2023) 123809

Contents lists available at ScienceDirect

Talanta

journal homepage: www.elsevier.com/locate/talanta

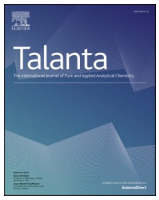

Evaluation of indirect sequence-specific magneto-extraction-aided LAMP for fluorescence and electrochemical SARS-CoV-2 nucleic acid detection

Sayantan Tripathy [a,b,d,1], Tanvi Agarkar [c,1], Arunansu Talukdar [e], Mrittika Sengupta [b,d], Ashvani Kumar [c,f,**], Souradyuti Ghosh [a,b,d,g,*]

[a] Department of Chemistry, Bennett University, India
[b] Department of Biotechnology, Bennett University, India
[c] Department of Physics, Bennett University, India
[d] Center of Excellence for Nanosensors and Nanomedicine, Bennett University, India
[e] Geriatric Medicine Department, Medical College and Hospital, Kolkata, India
[f] Pristine Diamonds Pvt. Ltd, Vatva, India
[g] Division of Radiation and Stress Biology, UGC-DAE CSR Kolkata Centre, Kolkata, India

ARTICLE INFO

Keywords:
Magnetic sequence-specific target enrichment
Quantitative real-time LAMP
Electrochemical LAMP
SARS-CoV-2

ABSTRACT

Nucleic acid amplification tests (NAATs) such as quantitative real-time reverse transcriptase PCR (qRT-PCR) or isothermal NAATs (iNAATs) such as loop-mediated isothermal amplification (LAMP) require pure nucleic acid free of any polymerase inhibitors as its substrate. This in turn, warrants the use of spin-column mediated extraction with centralized high-speed centrifuges. Additionally, the utilization of centralized real-time fluorescence readout and TaqMan-like molecular probes in qRT-PCR and real-time LAMP add cost and restrict their deployment. To circumvent these disadvantages, we report a novel sample-to-answer workflow comprising an indirect sequence-specific magneto-extraction (also referred to as magnetocapture, magneto-preconcentration, or magneto-enrichment) for detecting SARS-CoV-2 nucleic acid. It was followed by in situ fluorescence or electrochemical LAMP. After in silico validation of the approach's sequence selectivity against SARS-CoV-2 variants of concern, the comparative performance of indirect and direct magnetocapture in detecting SARS-CoV-2 nucleic acid in the presence of excess host nucleic acid or serum was probed. After proven superior, the sensitivity of the indirect sequence-specific magnetocapture in conjunction with electrochemical LAMP was investigated. In each case, its sensitivity was assessed through the detection of clinically relevant 10^2 and 10^3 copies of target nucleic acid. Overall, a highly specific nucleic acid detection method was established that can be accommodated for either centralized real-time SYBR-based fluorescence LAMP or portable electrochemical LAMP.

1. Introduction

The upsurge of novel coronavirus disease (COVID-19), caused by the severe acute respiratory syndrome-2 virus (SARS–CoV-2), has led to 510 million infections and 6.2 million deaths (as of April 26, 2022) [1]. The SARS-CoV-2 RNA could be detected via the quantitative reverse transcription-polymerase chain reaction (qRT-PCR), a high specificity and sensitivity method using molecular targets present in their genome [2]. Despite the availability of several commercial qRT-PCR kits, it has several disadvantages. It requires a spin-column mediated pure nucleic acid extraction from the biological samples. This increases the overall turnaround time (TAT), cost, and the need for a high-speed centrifuge

Abbreviations: hgDNA, human genomic DNA; LAMP, Loop-mediated isothermal amplification; SYBR Green I, N,N-dimethyl-N'-[4-[(E)-(3-methyl-1,3-benzothiazol-2-ylidene)methyl]-1-phenylquinolin-1-ium-2-yl]-N'-propylpropane-1,3-diamine; qRT-PCR, quantitative real-time reverse transcriptase PCR; qLAMP, quantitative real-time LAMP; qRT-LAMP, quantitative real-time reverse transcriptase LAMP; eLAMP, electrochemical end-point LAMP; eRT-LAMP, electrochemical reverse transcription end-point LAMP; NAAT, nucleic acid amplification technique; iNAAT, isothermal nucleic acid amplification technique; VTM, viral transmission media; TAT, turnaround time; near-POC, near-point-of-care.

* Corresponding author. Department of Chemistry, Bennett University, India.
** Corresponding author. Department of Physics, Bennett University, India
E-mail addresses: ashuiit19@gmail.com (A. Kumar), souradyutighoshacademic@gmail.com (S. Ghosh).
[1] joint first author.

https://doi.org/10.1016/j.talanta.2022.123809
Received 27 April 2022; Received in revised form 27 July 2022; Accepted 1 August 2022
Available online 12 August 2022

present in a centralized lab. Additionally, a separate reverse transcription step is often required as few existing kits integrate the reverse transcription with the real-time PCR step. In fact, single-step qRT-PCR has lower sensitivity than that of two-step assays [3,4]. The multi-step assays necessitate the recruitment of trained workforce for conducting them. Furthermore, the possible presence of host nucleic acid requires a sequence-selective TaqMan probe, adding to the cost.

Thermal-cycler-independent isothermal nucleic acid amplification techniques (iNAATs) such as reverse transcription loop-mediated isothermal amplification (RT-LAMP) have been deployed in one-step SARS-CoV-2 detection using colorimetric as well as fluorescence readouts [5–7]. Additionally, a LAMP amplicon could also be quantified by end-point electrochemical detection [8]. Besides quantitative readouts in the centralized laboratory, the latter feature could be utilized for near-point-of-care (near-POC) diagnostics in a resource-limited area [8]. Despite such advantages, most LAMP assays require prior RNA extraction from viral transmission media (VTM). Few studies have so far bypassed or integrated nucleic acid extraction with downstream in situ LAMP or other NAAT [9]. Rather than using direct amplification from clinical or simulated samples, most LAMP-based bioanalytical methods utilized pre-extracted nucleic acid or in situ purifications. On the other hand, NAATs using non-extracted nucleic acid as a template significantly reduced the specificity and sensitivity for SARS-CoV-2 detection and may not work at all with SYBR-based qRT-PCR [10]. The clinical sensitivity and specificity of reverse transcription LAMP (RT-LAMP) also decrease significantly when non-extracted RNA has been used as a template (sensitivity reducing from 97% to 71% and specificity from 100% to 47%, for pre-extracted and non-extracted RNA templates, respectively) [11]. In another study, direct colorimetric LAMP using non-extracted RNA from saliva samples generated false positive readouts [12]. Similarly, direct colorimetric RT-LAMP on the untreated clinical sample detected SARS-CoV-2 RNA only when the viral copy number was above 3000 copies/μL. With RNase inactivation or combined RNase inactivation and extraction, the analytical sensitivity improved to 25 copies/μL and 2.5 copies/μL, respectively [13]. Besides, SARS-CoV-2 detection has surprisingly not been conducted yet using electrochemical LAMP readouts, despite their utility in the near-POC settings.

A sequence-specific preconcentration employs sequence complementarity of a probe oligonucleotide to a target nucleic acid. Using either solid phase or magnetic bead-based immobilization of the probe oligonucleotide, unwanted biomolecules such as polymerase inhibitors could be removed from the sample of interest. A sequence-specific magnetic preconcentration is advantageous due to its minimal equipment necessity, the possible scope of in situ amplification, lesser TAT, and reduced cost [14–16]. Due to its selectivity of target nucleic acid, it would (in principle) eradicate the need for TaqMan-like sequence-selective reporters in the downstream NAAT compared to whole nucleic acid extraction methods. Such assays, in combination with electrochemistry-mediated readout, would be advantageous in near-POC diagnostics in limited-resource settings. The sequence-specific capture could be direct or indirect in nature. In the direct capture, a magnetic bead-immobilized sequence-specific probe exploits complementarity to extract target nucleic acid [16]. The indirect magneto-enrichment utilizes a sequence-specific probe to first bind to the target of interest prior to magnetic bead immobilization. Due to the absence of a blocking step, it could however become susceptible to carryover contamination [17]. Despite the potential advantage, possibly higher sensitivity, and utility of sequence-specific magneto-enrichment, a comprehensive literature search of magnetic extraction methods combined with LAMP tabulated in Table S1 yielded only four direct magneto-enrichment studies (entries 20, 23, 43, 46) [16,18–20]. All four utilized microfluidic setup, requiring costly flow-controller equipments. The rest predominantly are either whole nucleic acid extraction (includes all SARS-CoV-2 detections, entries 7, 10, 14, 24, 35, 48, [21–26]), or immunomagnetic capture-lysis. Surprisingly, none of the studies utilized electrochemical readout despite its promising potential in limited resource detection or employed indirect sequence-specific magneto-enrichment. Therefore, the modality of an indirect magneto-enrichment of pathogen nucleic acid from a complex biofluid or host nucleic acid-containing sample with downstream LAMP, either with fluorescence or electrochemical readout, remains unexplored.

This work aims to establish a minimally instrument-intensive sample-to-answer workflow for selectively extracting target nucleic acid from samples containing complex biofluid and host nucleic acid, followed by an iNAAT assay. With this goal, the performance of an indirect sequence-specific magneto-extraction followed by fluorescence (SYBR-based) and electrochemical LAMP was probed. The experiment used SARS-CoV-2 *RdRp* plasmid DNA and RNA as analytes. In doing so, the effectiveness of direct and indirect sequence-specific magneto-extraction using quantitative real-time LAMP (qLAMP) was investigated. Their performance in a real-life-mimicking scenario was compared by detecting SARS-CoV-2 *RdRp* plasmid DNA from samples containing excess human genomic DNA (hgDNA) and serum. The superior one, the indirect magneto-extraction, was then integrated with electrochemical end-point LAMP (eLAMP) to detect SARS-CoV-2 nucleic acid from the real-life-simulating hgDNA and serum-spiked samples. In these experiments, we have established a flexible (compatible with fluorescence and electrochemical readout) yet sensitive pathogen nucleic acid detection method. Additionally, we also analyzed the effect of potential contaminants from serum and hgDNA on the performance of direct and indirect magnetocapture combined with downstream LAMP.

2. Experimental

2.1. Materials

Escherichia coli strK-12 substr. MG1655 plasmid construct with RNA-dependent RNA polymerase (*RdRp*) gene with T7 RNA polymerase promoter (4538 bp) was purchased from Addgene (plasmid #14567, https://www.addgene.org/145671/). The Bst 2.0 polymerase, RTx enzyme, dNTP, and SnaBI were procured from NEB, USA. The SYBR I (10,000X concentrated) was purchased from Invitrogen, USA. Molecular biology grade water was purchased from HiMedia, India. The RNase inhibitor was purchased from Takara. Streptavidin-coated magnetic beads were purchased from Sigma-Aldrich (# 11641778001) or Invitrogen (Dynabeads M − 280). 5′-biotinylated probe having the b sequence (5'-[BIO]-AAA AAA AAA ACG AGC AAG AAC AAG TGA GGC CAT AAT TC, HPLC purified, $T_m = 57.6$ °C at 50 mM NaCl and 0.25 μM oligonucleotide concentration) was purchased from Sigma-Aldrich. Primer oligonucleotides (desalting purified) were purchased from Eurofin or Sigma-Aldrich, India.

2.2. LAMP reaction and primer optimization using real-time fluorescence readout

A real-time quantitative LAMP (qLAMP) experiment was performed on 10^3 copies of ORF1ab containing plasmid with three sets of primer-sThe final LAMP reaction (20 μl) contained the three primer pairs in the following final concentrations: 0.2 μM outer primers, 1.6 μM forward and backward inner primers, 0.8 μM forward and back loop primers (for primer sets 1 and 3) [27,28]. For primer set 2, 0.4 μM outer primers, 0.332 μM forward and backward inner primer, 1 μM forward loop primers, and 0.4 μM back loop primers were utilized in the final concentration [29]. The reaction mixture also contained 2.0 μL of 10 × Bst 2.0 DNA polymerase reaction buffer [1 × containing 20 mM Tris-HCl, 50 mM KCl, 10 mM $(NH_4)_2SO_4$,2 mM $MgSO_4$, 0.1% Tween-20, pH 8.8], 1.4 mM dNTPs, 2.0 μL SYBR I (final concentration 1X diluted from 10,000X stock), 0.5 μL of an 8 U μl concentration of Bst 2.0 DNA polymerase, 6 mM $MgSO_4$ and 1 μl template (alternatively, 2 μL magnetic bead for magnetocapture assays). For quantitative real-time reverse transcription LAMP (qRT-LAMP), 7 U (0.25 μL) of reverse transcriptase

RTx (NEB) was additionally added to the above. The qLAMP (or qRT-LAMP) reaction was set at the following settings for each cycle with a fluorescence monitoring step, 65 °C for 1 min for primer set 1, 64 °C for 1 min for primer set 2, 60 °C for 1 min for primer set 3 followed by thermal melting analysis step. The cycles were repeated 60 times (unless otherwise stated) in a CFX Maestro or CFX Connect real-time PCR (rt-PCR) machine (BioRad).

2.3. Electrochemical LAMP (eLAMP) assays

For eLAMP or eRT-LAMP using the pure nucleic acid template, the assay was performed on 10^1–10^4 copies of nucleic acid (*RdRp* plasmid DNA or *RdRp* RNA)/25 μL of reaction. For magnetocapture followed by eLAMP or eRT-LAMP assays, 2 μL magnetic beads containing immobilized target nucleic acid were added to 25 μL electrochemical LAMP reaction having a composition as described below. A 25 μL eLAMP or eRT-LAMP reaction comprised of 2.5 μL of 10 × Bst 2.0 DNA polymerase reaction buffer [1 × containing 20 mM Tris-HCl, 50 mM KCl, 10 mM $(NH_4)_2SO_4$, 2 mM $MgSO_4$, 0.1% Tween-20, pH 8.8], 1.4 mM dNTPs, 0.4 μM outer primers, 0.332 μM forward and backward inner primer, 1 μM forward loop primers, 0.4 μM back loop primers (primer set 2), 0.5 μL Bst 2.0 polymerase, and 50 μM methylene blue. During magnetocapture followed by eLAMP or eRT-LAMP, 1000 copies of non-magnetocaptured plasmid DNA or RNA was used as the positive control. For eRT-LAMP, 7 U of reverse transcriptase (RTx) was also used for 25 μL of reaction. The assays were set at the following settings for each cycle, 64 °C for 1 min for 60 cycles followed by heat inactivation at 80 °C for 20 min in a thermal cycler (Eppendorf). The resultant LAMP amplicons were electrochemically analyzed.

2.4. Method of plasmid digestion & in vitro transcription

1 μg target plasmid was linearized with 1 μL SnaBI enzyme (10 U/μL) and 1X NEB CutSmart buffer (50 mM Potassium Acetate, 20 mM Tris-acetate, 10 mM Magnesium Acetate, 100 μg/ml BSA pH 7.9 at 25 °C) by incubating at 37 °C for 1 h (final volume 50 μL). Next, the digestion was stopped by an additional enzyme inactivation step (80 °C for 20 min). Next, 4 μL of the digested sample was loaded into 2% agarose gel to check the linearized product. 1 μg of digested plasmid was then added with 1X NTP buffer mix (NEB), 2 μL of T7 RNA polymerase in 20 μL reaction, and incubated at 37 °C for 2 h. The resultant RNA product was cleaned with Monarch® RNA Cleanup Kit (NEB) as per the manufacturer's instruction. Briefly, 100 μL of RNA clean-up binding buffer was added to the 50 μL sample obtained from the reaction. 150 μL of pure ethanol is added to the mixture and loaded into the column provided in the kit. After centrifugation at 13000 rpm for 1 min, the column is again washed with 500 μL wash buffer, and finally, the product was eluted in 50 μL nuclease-free water.

2.5. Method of RNA quantification by qPCR

cDNA was synthesized using the PrimeScript 1st strand cDNA Synthesis Kit (Takara) as per the manufacturer's instruction. Briefly, 1 μg RNA was mixed with 0.4 μL random hexamers, 1 mM dNTP mixture, and snap cooled (65 °C for 5 min, followed by incubation in ice for 5 min, final volume 10 μL). Then, cDNA was synthesized with 1X prime script buffer, 100 U of reverse transcriptase, and template RNA primer mixture and was incubated at 30 °C for 10 min followed by 50 °C for 30 min (final volume 20 μL total). Parallelly, a standard curve for copy numbers vs C_t value was generated by qPCR on plasmid DNA. The qPCR was performed to determine the cDNA concentration and analyzed using a CFX Maestro (BioRad) with SYBR Green Real-Time PCR Master Mix Plus (HiMedia) followed by thermal melting analysis. The primers were designed against the *RdRp* gene of the plasmid (Eurofins, please see sequences in Table S3). The cDNA was diluted 1/400 fold and subjected to qPCR to determine its concentration.

2.6. Direct sequence-specific magnetocapture followed by in situ LAMP

0.1 μM 5′-biotinylated probe oligonucleotide (having a b sequence) was first immobilized on the 10 μg streptavidin-coated magnetic nanoparticles by 20 min of incubation. After incubation with wash-binding buffer (5 mM Tris-HCl, 0.5 mM EDTA, 1 M NaCl, pH 7.5), the biotinylated probe-bound streptavidin-coated MNP was blocked with 1% BSA for 20 min. After three times of washing with wash-binding buffer, the probe-MNP complex was incubated (15 min, using vortex-enabled mild shaking) with snap-cooled (65 °C 5 min followed by cooling in ice for 5 min) 100 or 1000 copies of target plasmid carrying the *RdRp* gene (containing a b* sequence) in 40 μL 50 mM NaCl solution. For magnetocapture from hgDNA spiked sample, the plasmid was instead present in 40 μL 50 mM NaCl solution containing 1 ng MCF-7 extracted hgDNA and then subjected to magnetocapture as described. Similarly for serum-spiked samples, the plasmid was instead present in 40 μL 50 mM NaCl solution containing 10% (v/v, for DNA capture) serum. For the negative control (NTC), water is used instead of plasmid during the magnetocapture. After three successive washes using magnetic decantation with 200 μL wash-binding buffer, the target nucleic acid bound MNP was resuspended in 10 μL nuclease-free water. 2 μL beads were used for 20 μL in situ qLAMP reactions as described above.

2.7. Indirect sequence-specific magnetocapture followed by in situ LAMP

In this method, 0.1 μM 5′-biotinylated probe oligonucleotides having b sequence were first annealed with 100 or 1000 copies of target plasmid or *RdRp* RNA copies in 40 μL 50 mM NaCl solution by heating at 65 °C (2 min), followed by ice (5 min) and then 15 min benchtop incubation at room temperature. For magnetocapture from hgDNA spiked sample, the plasmid or RNA was instead present in 40 μL 50 mM NaCl solution containing 1 ng MCF-7 extracted hgDNA and then subjected to magnetocapture as described. Similarly, for serum-spiked samples, the plasmid or RNA was instead present in 40 μL 50 mM NaCl solution containing 10% (v/v, for DNA capture) or 5% (v/v, for RNA capture) serum (with or without the addition of RNase inhibitor and EDTA, see Supporting Information Section 8) and then subjected to magnetocapture as described (please see below for the protocol of RNA magnetocapture from RNase and EDTA treated serum). This step generates the plasmid (or RNA)-probe binary complex which was then followed by 15 min incubation (using vortex-enabled mild shaking) with 10 μg streptavidin-coated MNP at room temperature. For the negative control (NTC), the magnetocapture was performed with the same solution but lacking the target nucleic acid. After three times washes with wash-binding buffer using magnetic decantation, the target nucleic acid bound MNP has resuspended in 10 μl nuclease-free water. 2 μL beads were used for 20 μL in situ qLAMP/eLAMP as described above.

2.8. Method of magnetocapture of 100 and 1000 copies of in vitro transcribed RNA from 5% serum spiked solution

6.6% fetal bovine serum (Gibco), 1.0 μL of RNase inhibitor, 25 mM EDTA (final) are incubated together at 37 °C for 1 h to a final volume of 30 μL. 100 and 1000 copies of RNA in an aqueous solution (final volume 10 μL) were heated up to 65 °C for 2 min followed by the immediate addition of preincubated EDTA-serum mixture (above) and 0.1 μM (final concentration) of 5′-biotinylated probe oligonucleotides (sequence b) to a final volume of 40 μL and then cooled in ice. The rest of the magnetocapture procedure was identical to as described for indirect magnetocapture in the main manuscript.

2.9. Method of electrochemical measurement

The samples were tested electrochemically using commercially purchased screen-printed electrodes (SPE) with carbon, carbon, and silver as working, counter, and quasi-reference electrodes, respectively.

The electroanalytical study was performed via square-wave voltammetry (SWV) using Metrohm Autolab PGSTAT302 N potentiostat/galvanostat (with NOVA software for data analysis). The voltage was swept from a range of 0 to −1 V (scan rate 50 mV/s) for 5 consecutive cycles and the current was recorded simultaneously. The current intensity of the redox mediator would be measured at a potential (V) position of −0.32 V (before baseline correction, please see below). All the electroanalytical data presented were averaged over 4 cycles, excluding the first cycle since an intense current was observed in the first cycle due to the electrode's electric double layer (EDL) charging. Prior to data analysis, a baseline correction was done by drawing a straight line connecting the two extremes of the SWV curve using the NOVA software. The software then created a precise baseline for data analysis. The "absolute peak current" corresponded to the magnitude of the peak current irrespective of the sign after baseline correction. The absolute peak current is therefore the modulus of the obtained current peak value after baseline correction. The percent signal change (S(I)) was calculated using this formula,

$$S(I) = \frac{I_0 - I_1}{I_0} * 100 \ \ \%$$

Where I_0 and I_1 were the absolute peak current signals generated from samples corresponding to the NTC and target-containing samples, respectively.

3. Results and discussion

3.1. Use of plasmid construct containing SARS-CoV-2 RdRp gene and selection of LAMP primers

As per NIH Guideline for SARS-CoV-2 research, in vitro expression of partial viral RNA or protein from plasmid construct, or bacteria carrying such constructs would result in non-infectious products, permitting the experiments to be conducted under BSL-2 containment [30,31]. Accordingly, a plasmid expressing the SARS-CoV-2 RNA-dependent RNA polymerase (*RdRp*) gene and its in vitro transcribed RNA were utilized. Three published LAMP primer sets (see Supporting Information Section 2) against the *RdRp* gene were investigated in differentiating 10^3 copies of the plasmid from no template control (NTC) in a quantitative real-time LAMP (qLAMP) assay [29]. Among these, set 2 displayed the highest ΔC_t (C_t refers to cycle threshold) and was selected [29] (Fig. S1A and B). The qLAMP study performed on the serially diluted plasmid DNA template with primer set 2 detected the analytical sensitivity at 10 copies/reaction (Fig. S1C). The C_t values in the qLAMP reaction matched that of the original paper [29].

3.2. Probe design, sequence-specificity, and methodology of magnetocapture of SARS-CoV-2 RdRp plasmid followed by detection using qLAMP

Next, the utility of direct and indirect sequence-specific magnetocapture assay utilizing a biotinylated probe sequence for detecting *RdRp* plasmid DNA from 40 μL aqueous solution was investigated (Scheme 1). From 5′ to 3′, the probe contained a 5′-biotinylation site followed by a 10 nt polyA linker and the 28 nt target binding "b" region, respectively. The sequence alignment of the "reverse complement" of the target binding region of the probe showed full complementarity with SARS-CoV-2 strains isolate WIV04 (accession number MN996528.1) [32], Delta variant or B.1.617.2 (accession number OK091006.1) [33], and Omicron variant or B.1.1.529 (accession number OM570283.1) [34] (Fig. S2A – C). At the same time, 22 nt and 9 nt complementarity (out of 28 nt target binding region) were found against SARS-CoV-1 (accession number NC_004718) and the Middle East respiratory syndrome (MERS, accession number KT225476) coronaviruses, respectively (Fig. S2D and E) [35,36]. Next, we investigated the selectivity of probe-target annealed complex formation for SARS-CoV-2 and SARS-CoV-1 using NUPACK online software package (Table S3) [37]. When the target concentration was in the clinically relevant 1 pM or 1 fM range, the

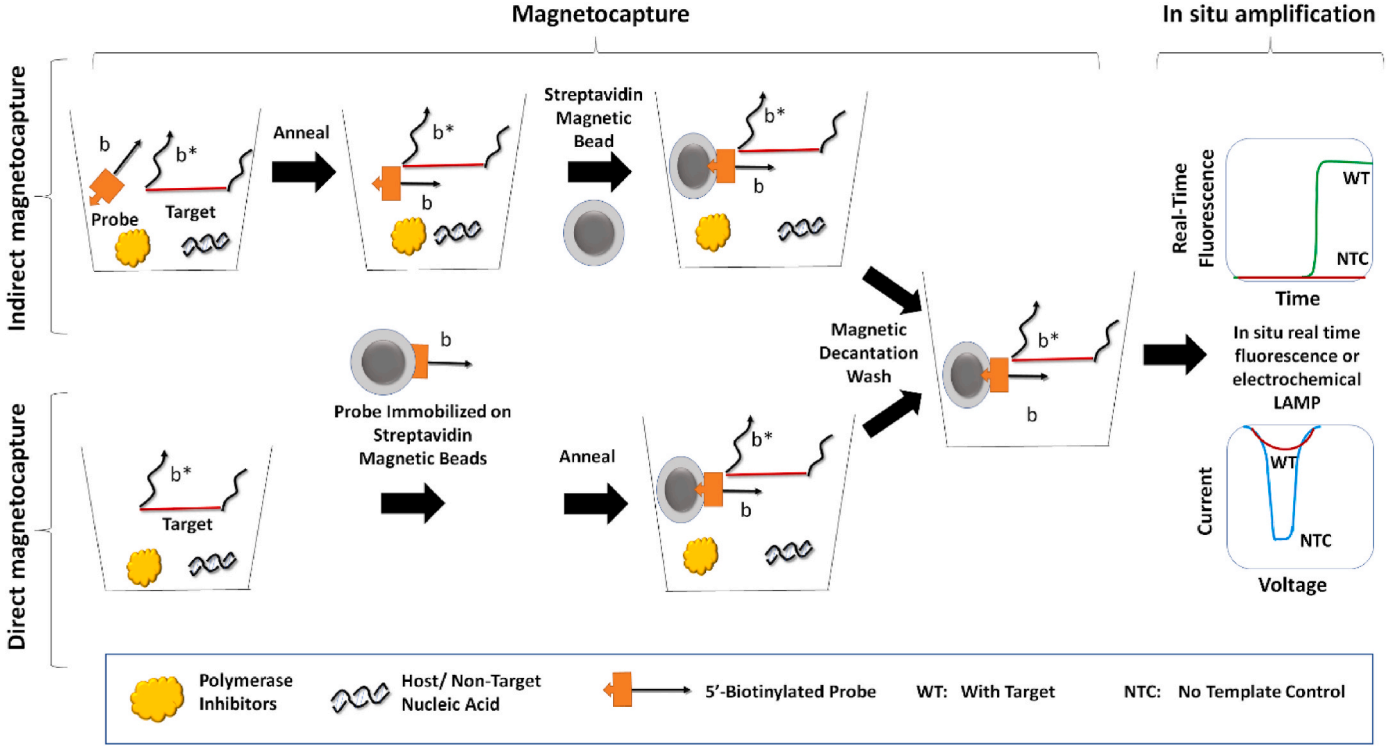

Scheme 1. Indirect and direct sequence-specific magnetocapture of target nucleic acid (present with host nucleic acid and polymerase inhibitors from serum) leads to probe-target nucleic complex immobilized on the magnetic bead. Following magnetic decantation wash, the target bound magnetic beads was used for in situ LAMP (or reverse transcriptase LAMP) amplification with fluorescence or electrochemical readout.

efficiency of probe-target complex formation could be unambiguously differentiated. In fact, the probe-target complex failed to generate for the 1 fM SARS-CoV-1 target concentration (equivalent to 24 × 10^3 copies in 40 μL solution), underscoring the method's selectivity. Due to already low sequence complementarity, the probe-target complex formation against MERS was not investigated. In addition to the target capture probe, the specificity of the LAMP primers is further anticipated to improve the selectivity of the proposed detection method.

For direct magnetocapture, a 5′-biotinylated probe oligonucleotide (having the target binding b sequence) was first immobilized on the streptavidin-coated magnetic beads. This was followed by blocking and then annealing with target nucleic acid carrying the *RdRp* gene (containing a b* sequence complementary to probe b, Scheme 1). In the indirect magnetocapture, the 5′-biotinylated probe oligonucleotide was first annealed with target nucleic acid followed by immobilization on streptavidin-coated magnetic beads (Scheme 1). In both cases, magnetic decantation wash (and resulting physical separation) then removed any polymerase inhibitors or non-target nucleic acid from the magnetic bead-bound probe-target complex. The direct and indirect magneto-extraction on target plasmid *RdRp* DNA were completed with 60 and 30 min assay times, respectively.

Next, the magnetic bead carrying the target-probe complex was subjected to in situ qLAMP to assess the capture effectiveness (Fig. 1A). Presence of SYBR Green I in the amplification master mix enabled the real-time monitoring of qLAMP assay. The assay effectiveness was investigated by detecting clinically relevant 10^2–10^3 copies of the target nucleic acid (*RdRp* plasmid DNA) [38]. For both direct and indirect capture, the no template control (NTC) assays were carried out with a blank sample (i.e., without target), magnetic decantation, and then qLAMP. The NTC experiments consistently did not generate any amplification curves by the 60th cycle (please see representative amplification plots in the Supporting Information). However, to perform Student's t-test, its C_t value was taken at 60. Additionally, internal target controls comprising pure 10^3 copies of *RdRp* plasmid were included in each assay. Overall, the assay time (including the in situ qLAMP step) was 2 h and 1.5 h for direct and indirect magnetocapture, respectively.

For direct magnetocapture (Fig. 1B, Fig. S3A), 10^2 and 10^3 copies of plasmids were detected at significantly higher cycle threshold values (C_t) compared to indirect capture (Fig. 1B, Fig. S3B and S5E). The indirect magneto-enrichment probably utilized the superior diffusion rate of the smaller biotinylated probe oligonucleotide (compared to the bulkier magnetic bead immobilized probe) in finding and annealing with the target nucleic acid. The indirect capture method has also demonstrated superior target binding for nucleic acid capture as well as antigen-antibody interaction in prior studies [17,39]. Besides, it validates another independent observation that the bead-immobilized complementary probe (similar to direct magnetocapture) took over 2 h to capture 70% target nucleic acid from the solution [40]. Additionally, indirect magnetocapture does not require blocking. It was therefore was faster, relatively inexpensive, and has reduced pipetting steps. However, due to the absence of blocking, indirect magnetocapture would risk non-specific carryover contamination from complex biofluids and host nucleic acid. To investigate this, the compatibility of indirect magnetocapture in detecting nucleic acid targets from human genomic DNA (hgDNA)-spiked and serum-spiked aqueous solution was explored.

3.3. Comparison of direct and indirect magneto-extraction for the detection of SARS-CoV-2 RdRp plasmid DNA from hgDNA- and serum-spiked samples

In clinical samples, the target nucleic acid may often remain mixed with polymerase inhibitors which might hinder downstream real-time PCR application [41]. The presence of hgDNA may sometimes interfere with the efficiency and specificity of downstream amplification. Serum, on the other hand, is also a component of viral transport media (VTM) and has polymerase inhibitory property due to the presence of heme and immunoglobulin proteins [41,42]. Therefore, detecting the target nucleic acid from samples spiked with host nucleic acid or serum would simulate the assay performance in a real-life scenario. To investigate, 10^2–10^3 copies of the target *RdRp* plasmid (1–10 fg, respectively)

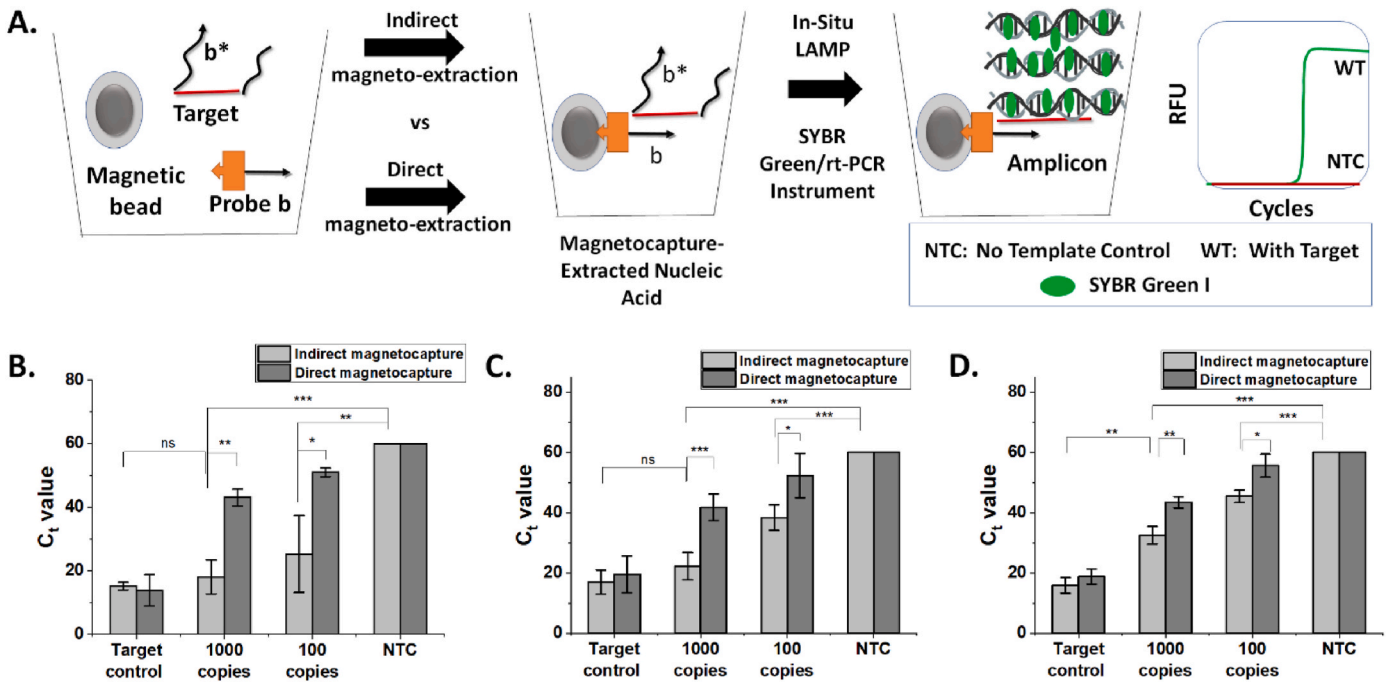

Fig. 1. Comparison of indirect and direct sequence-specific magnetocapture of 100 copies (1 fg) and 1000 copies (10 fg) of SARS-CoV-2 *RdRp* plasmid DNA from aqueous solution (Panel B), and solutions spiked with 1 ng hgDNA (Panel C), or serum (10%, v/v, Panel D) followed by in situ qLAMP. Panel A describes the scheme of in situ qLAMP with magnetocaptured SARS-CoV-2 *RdRp* plasmid DNA. Target control LAMP experiments were performed with 10^3 copies of pure plasmid DNA (without any magnetocapture). NTC assays comprised of magnetocapture experiments that were carried out without any target nucleic acid followed by qLAMP. Error bars represent standard deviation (n = 3). *P ≤ 0.05, **P ≤ 0.01, ***P ≤ 0.001, ****P ≤ 0.0001.

in 40 μL spiked with excess hgDNA (1 ng) or 10% fetal bovine serum (FBS) samples were subjected to direct and indirect sequence-specific magnetic preconcentration followed by in situ qLAMP with an SYBR Green containing mastermix (Fig. 1A). Accordingly, NTC magneto-capture experiments also included the same samples albeit free of *RdRp* plasmid. Compared to aqueous samples (above), direct magneto-extraction detecting 10^2 and 10^3 copies of *RdRp* plasmid demonstrated similar C_t values. However, indirect capture showed slightly higher C_t values compared to its aqueous counterpart (Fig. 1C and D, Fig. S4 and S5). We plotted the change of C_t value (ΔC_t) between direct and indirect magnetocapture for aqueous, hgDNA- and serum-spiked samples for 10^2 and 10^3 copies to gauge their relative efficacy (Figure S5E). It demonstrated that similar to the aqueous sample, the indirect magnetic preconcentration demonstrated better efficacy (compared to direct capture) for hgDNA-spiked and serum-spiked samples as well. The slight increase in C_t value for the indirect magneto-extraction-amplification for the hgDNA- and serum-spiked samples (compared to aqueous solution) could be attributed to possible carryover contamination (Figure S5F). These experiments thus conclusively validated the superiority of indirect sequence-specific magneto-enrichment-assisted qLAMP for detecting 10^2–10^3 copies of *RdRp* plasmid DNA (i.e., 2.5–25 copies/μL or 4.1–41 aM) from real-life mimic samples. Although the target nucleic acid was double-stranded, direct sequence-specific capture of double-stranded genomic DNA has been achieved before [16,18–20]. It probably occurred through localized denaturation followed by probe binding. Similar to aqueous samples, the sample-to-answer TAT for the indirect magneto-enrichment-amplification assay was 1.5 h.

3.4. Detection of SARS-CoV-2 RdRp RNA spiked with hgDNA and serum

Due to the better efficacy of indirect sequence-specific magneto-enrichment-assisted qLAMP, it was then utilized in detecting SARS-CoV-2 *RdRp* RNA (in vitro transcribed from plasmid). The in vitro transcription, characterization, and quantification of RNA containing *RdRp*, and standard curve generation for quantitative real-time reverse transcription LAMP (qRT-LAMP) assay (using pure RNA) have been described in the Supporting Information Section 6, Fig. S6 and S7. Like *RdRp* plasmid DNA, the qRT-LAMP involving pure *RdRp* RNA could sense 10 copies/reaction with four orders of dynamic range and similar C_t values as the plasmid (Fig. S7). Next, the detection of 100–1000 copies of *RdRp* RNA present in 40 μL aqueous media, hgDNA spiked aqueous solution, or serum-spiked sample was carried out using indirect capture of *RdRp* plasmid followed by one step in situ qRT-LAMP (Scheme 1 and Fig. 2). For the magneto-enrichment of RNA from the aqueous sample, 100–1000 copies of target RNA were detected with marginally higher C_t compared to indirect *RdRp* plasmid capture from the aqueous sample (Fig. 2B, Fig. S8A and C). Similarly, for the samples containing hgDNA, 100–1000 RNA copies were detected with slightly higher C_t compared to aqueous indirect magneto-enrichment (Fig. 2C, Fig. S8B and D). This result suggests that proposed magneto-enrichment-assisted in situ qRT-LAMP detection would be possible in the presence of hgDNA, therefore bypassing the need for the TaqMan probe. The higher C_t value for hgDNA spiked samples could result from lesser effectiveness in target capture specificity due to the presence of excess (10^5 times higher in weight) of hgDNA.

Next, the detection of RNA present in serum-spiked (5%, v/v) sample was investigated. Due to the presence of 0.5–5% serum in VTM [43,44], this experiment's efficacy would be predictive of the performance of the indirect magnetocapture in an actual clinical sample. Due to RNase activity and the presence of polymerase inhibitors, the analytical sensitivity of an SYBR I-based qRT-PCR and RT-LAMP without RNA extraction was significantly lower than that involving pre-extracted RNA [10–13]. We also initially encountered significant target RNA degradation when attempting magneto-extraction on a 5% untreated serum-spiked sample. Therefore, we added RNase inhibitor and EDTA to

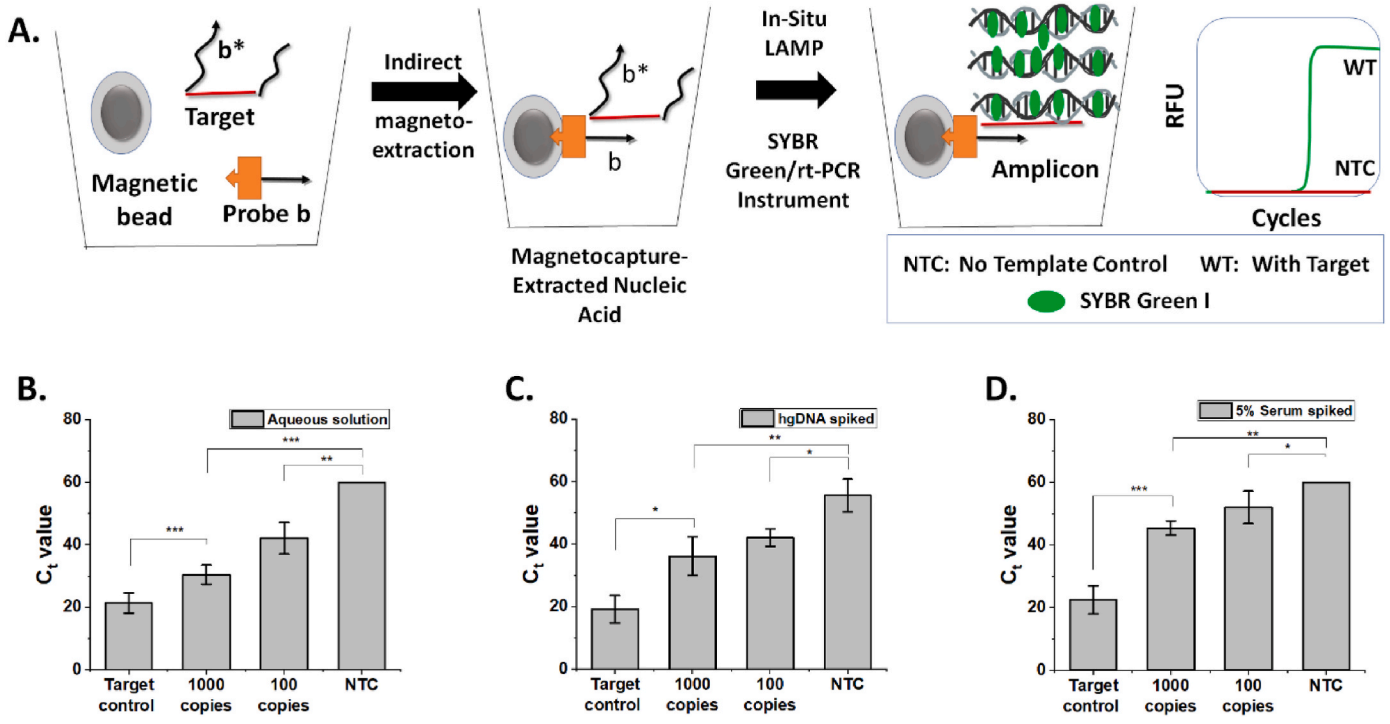

Fig. 2. Indirect magnetocapture of 100 and 1000 copies of in vitro transcribed SARS-CoV-2 *RdRp* RNA from aqueous media (Panel B), or aqueous sample spiked with hgDNA (1 ng, Panel C), or serum (5%, v/v, Panel D) followed by in situ qRT-LAMP. Panel A describes the scheme of in situ qRT-LAMP with magnetocaptured SARS-CoV-2 *RdRp* RNA. Target control qRT-LAMP experiments were performed with 10^3 copies of *RdRp* RNA (without any magnetocapture). NTC assays comprised of magnetocapture experiments that were carried out without any target RNA followed by qRT-LAMP Error bars represent standard deviation (n = 3). *P ≤ 0.05, **P ≤ 0.01, ***P ≤ 0.001, ****P ≤ 0.0001.

prevent RNA degradation in this sample as described in Supporting Information sections 8 and 9. The C_t values in serum spiked samples were relatively higher (56.2 ± 7.7 and 47.3 ± 2.2 for 100 and 1000 copies, respectively) compared to RNA detection from aqueous media or hgDNA spiked sample (Fig. 2D). This was probably due to the continued degradation of some target RNA and would cause a longer TAT (2.0 h, Fig. 2D, Fig. S10). Despite the stated addition of RNase and EDTA, the proposed magnet-extraction could not successfully detect RNA from a 10% serum-spiked solution, presumably due to significant RNA degradation (not shown). Nevertheless, our method detected clinically relevant 100 copies of SARS-CoV-2 *RdRp* RNA (2.5 copies/μL or 4.1 aM) from aqueous and hgDNA-spiked samples and 1000 copies (25 copies/μL or 41 aM) from serum-spiked samples.

3.5. Detection of SARS-CoV-2 plasmid DNA and RNA using sequence-specific indirect magneto-extraction and electrochemical LAMP

Next, the detection of *RdRp* plasmid DNA or RNA using the indirect magneto-extraction integrated LAMP using electrochemical end-point LAMP (eLAMP) or electrochemical reverse transcription end-point LAMP (eRT-LAMP) was probed. The studies were carried out on a carbon (working electrode)-carbon (counter electrode)-silver (quasi reference electrode) screen-printed electrode, with methylene blue as the redox indicator, and square wave voltammetry (SWV) as the electroanalytical method. If demonstrated a similar analytical sensitivity as that of real-time fluorescence, the electrochemical detection of NAATs would ultimately be advantageous as it facilitates nucleic acid-sensing without bulky real-time PCR instruments. The methylene blue was utilized as the redox mediator due to its proven superiority over others such as sodium molybdate or osmium tetroxide [45]. Similarly, SWV was applied due to its greater sensitivity thanks to minimal capacitive as well as background currents. Positively charged methylene blue binds to the negatively charged nucleic acid backbone using electrostatic interaction and intercalation in a sequence-independent manner [46]. The presence of an amplicon would sequester the available methylene blue in solution, preventing electron transfer to the electrode, thereby reducing the current signal (Fig. 3A). Additionally, an increasingly greater amount of template copies present in the reaction would generate a higher amount of amplicon, trapping more methylene blue, causing a successively lesser current transfer to the electrode and decreasing signal generation (Figure S11A and B). Accordingly, the peak current (current signal calculated after baseline correction, please see Materials and Methods section 2.9) would indicate the amplification's magnitude. The same results could alternatively be observed through the increasing magnitude of the signal % change ($S(I) = (I_0 - I_1) \times 100/I_0$), where I_0 and I_1 were the peak current signals generated from samples corresponding to the NTC and target containing samples, respectively), representing the relative change in the current signal compared to the NTC samples.

Accordingly, eLAMP or eRT-LAMP assay involving pure 10^1–10^4 copies of DNA and RNA showed a gradually decreasing peak current signal and a progressively increasing signal % change (Fig. 3B and C, Figure S11C and D). Considering a 5% absolute current signal change to NTC as the threshold, the analytical sensitivity for electrochemical LAMP on pure DNA and RNA were 10 and 100 copies, respectively (Figure S11C and D). Next, we performed the magnetocapture of clinically relevant 100 and 1000 copies of plasmid DNA and RNA from aqueous, hgDNA spiked, and serum spiked samples [38]. A consistent difference in peak current signal (compared to NTC) of 8–18 μA and 7–15 μA validated the compatibility of indirect magneto-extraction with eLAMP (Fig. 4B and C). Similarly, the peak current signal % change between NTC and 100–1000 copies of the plasmid and RNA reproducibly remained in the range of 11–26% and 11–32% respectively (Fig. S12A and B). Despite this validation, the magneto-extraction LAMP assays could not distinguish between magnetocaptured 100–1000 copies of nucleic acid, an aspect to be improved in future developments (please see below for rationalization). Overall, the indirect magneto-enrichment followed by eLAMP successfully demonstrated the detection of clinically relevant 2.5 copies/μL (100 copies in 40 μL or 4.1 aM) of target SARS-CoV-2 nucleic acid with a sample-to-answer TAT of 2 h from hgDNA and serum-spiked samples. It also reflected a similar performance as that of qLAMP-mediated detection.

3.6. Comparison of LAMP using a pure nucleic acid template and indirect magneto-extraction assisted LAMP

In this section, we have explored a comparison between qLAMP and eLAMP using the pure template and also weighed their performance against the indirect magneto-extraction-assisted qLAMP or eLAMP. It may appear that the C_t values for indirect magneto-extraction-assisted LAMP are significantly higher (and even outside the range of qLAMP standard curves shown in Fig. S1 and Fig. S7) than qLAMP using the pure template. However, the in situ 20 μL qLAMP was performed using only 1/5th of the magnetic beads (2 μL) from magneto-extraction. This was because adding more (>2 μL) beads in a 20 μL reaction inhibited the qLAMP (data not shown). In situ amplification of the entire 10 μL bead from the magnetocapture therefore would necessitate proportionately increasing reaction volume to 100 μL. In that case, a substantially lower C_t value of the magneto-extraction-assisted qLAMP could be anticipated, although this would increase the assay cost (see section 3.7 for an estimate).

Another interesting observation was that the end-point current signal from eLAMP (or eRT-LAMP) was non-differentiable for 100 and 1000 copies of magneto-extracted target nucleic acids. This could also be because the eLAMP quantifies the current at the end of the LAMP

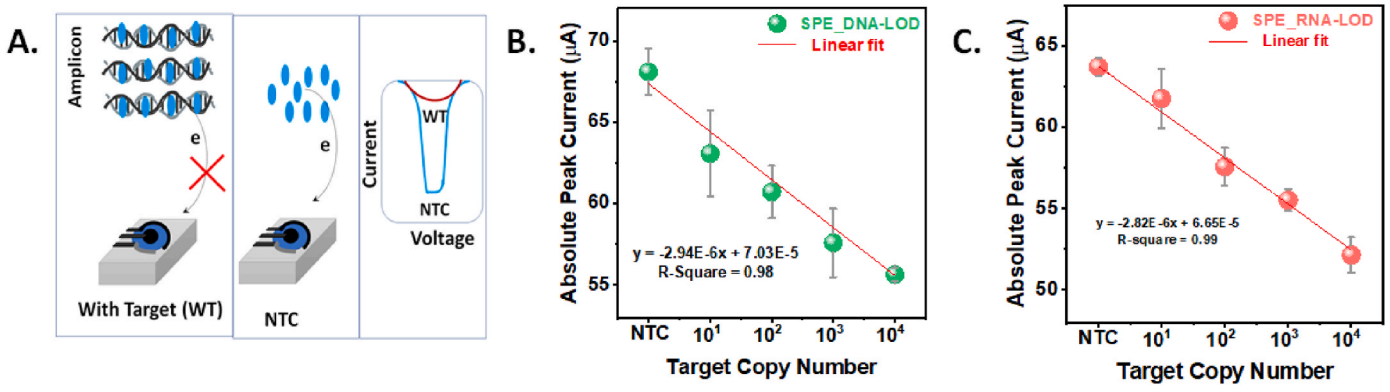

Fig. 3. Electrochemical LAMP studies conducted on pure 10^1–10^4 copies of SARS-CoV-2 *RdRp* plasmid DNA (Panel B) or RNA/reaction (Panel C) (without magnetocapture). Panel A describes the mechanism of amplicon-mediated methylene blue sequestration and subsequent reduction of current. NTC assays were conducted without any template nucleic acid addition. (For interpretation of the references to color in this figure legend, the reader is referred to the Web version of this article.)

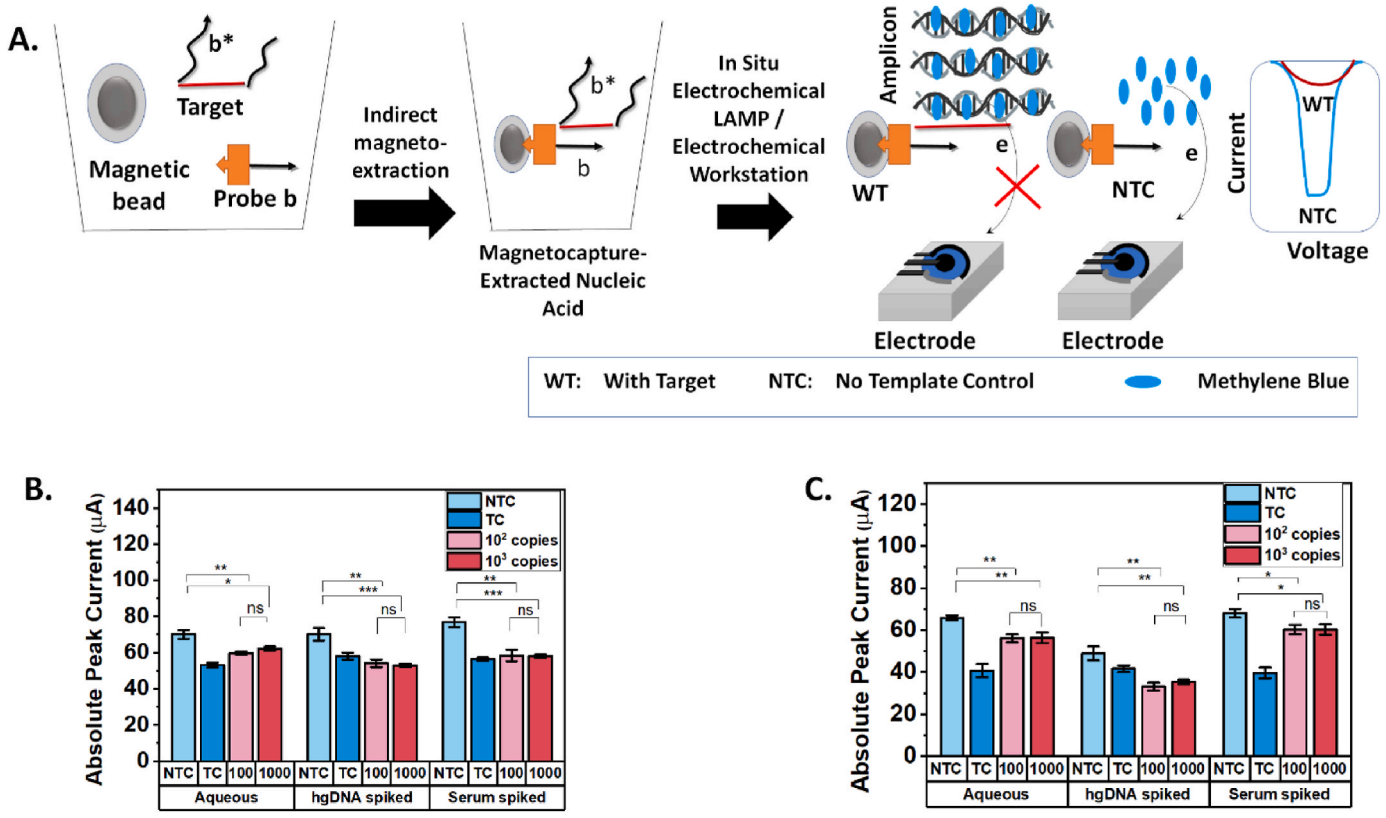

Fig. 4. Indirect magnetocapture of 100 and 1000 copies of SARS-CoV-2 *RdRp* plasmid DNA (Panel B) and RNA (Panel C) from aqueous media, aqueous sample spiked with hgDNA (1 ng), or serum followed by in situ electrochemical endpoint (reverse transcription) LAMP (eLAMP or eRT-LAMP). Panel A describes the scheme of in situ eLAMP with magnetocaptured 100 and 1000 copies of SARS-CoV-2 *RdRp* plasmid DNA or RNA. Target control (TC) eLAMP or eRT-LAMP experiments were performed with 10^3 copies of *RdRp* DNA or RNA, respectively (without any magnetocapture). NTC assays comprised of magnetocapture experiments that were carried out without any target DNA or RNA followed by eLAMP or eRT-LAMP, respectively. Error bars represent standard deviation (n = 3). *P ≤ 0.05, **P ≤ 0.01, ***P ≤ 0.001, ****P ≤ 0.0001.

reaction. Its measurement would therefore be proportional to the total amount of amplicon presence in the experiment. An assessment of the representative fluorescence amplification curves thus revealed that the end-point fluorescence (at the 60th cycle), representing total amplicon, was in the order of 800–1000 RFU (Fig. S3B, S5A and B, S8A and B), and thus might rationalize this observation. These factors, either individually or in combination with a homemade mastermix, may have led to a non-distinguishable current signal between magneto-extracted 100 and 1000 copies of target nucleic acid. Either stopping the LAMP reaction earlier or using a different primer set with even higher specificity could also help detect and differentiate close copy numbers of viral nucleic acid.

3.7. Discussion, comparison with published reports, cost, and future studies

In this work, we have circumvented the necessity of pure nucleic acid templates, and thermal cycling in NAAT and iNAAT methods by exploring indirect sequence-specific magneto-extracted assisted LAMP. The proposed assay successfully demonstrated proof-of-concept detection of clinically relevant 100–1000 copies (equivalent to 2.5–25 copies/μL) SARS-CoV-2 *RdRp* plasmid DNA and RNA from aqueous, hgDNA spiked, and serum spiked VTM-simulating samples. For the studies listed in Table S1, the limit of detection of the magneto-extraction assisted LAMP for SARS-CoV-2 detection are 4.2 copies/reaction [22], 3.7 copies/μL [24], 25 copies [25], and 20 copies [26]. Therefore, the performance of the proposed method has been equivalent to or superior to other published magnetocapture-assisted extraction assays. Its analytical performance at 2.5–25 copies/μL detectability was vastly superior to direct RT-LAMP performed on non-extracted RNA present in clinical samples (limit of detection 3000 copies/μL) [13]. The proposed assay has a comparable performance when compared with RT-LAMP performed on RNase treated, and silica-bead extracted RNA template and qRT-PCR (both reporting limit of detection at 2.5 copies/μL) [13].

When assessed for cost benefits, the cost of the raw materials in our method was INR 224 or $3.04 per assay (involving all commercial reagents, Table S4) with TAT in 2–2.5 h. In comparison, the spin-column or magnetic bead-based RNA detection kits (inclusive of extraction and amplification module) would cost $6–11/sample with TAT (sample-to-answer) ranging from 4 h to 1 day [10,47]. While automated cartridges integrate the whole sample-to-answer in a 1–1.5 h single continuous workflow, they are also costlier (over $10 per assay) [48]. This implied that our integrated indirect magnetocapture amplification would be inexpensive than existing RNA extraction and qRT-PCR kits despite the faster and limited-resource-friendly detection. With in-house prepared magnetic beads and enzymes, the assay cost could be expected to go down even further. Given the general nature of detection and low assay cost, this method could also sense any target pathogen nucleic acid and is therefore expected to see broader applications in the future. We are currently optimizing its applicability with clinical samples, lateral flow assay readouts, and a microfluidic set up.

4. Conclusion

This work addressed several critical issues currently concerning the NAAT and isothermal NAAT molecular diagnosis, namely, the requirement of nucleic acid extraction to remove polymerase inhibitors, the use of sequence-selective reporter probes for specificity, thermal cycling,

and the requirement of a centralized real-time PCR machine. Here, we have developed a comprehensive sample-to-answer workflow comprising an indirect sequence-specific magneto-preconcentration combined with LAMP for detecting an ultralow quantity of nucleic acid analytes present in aqueous as well as real-life simulating hgDNA- or serum-spiked samples. Utilizing downstream real-time SYBR-based fluorescence and electrochemical end-point readout, the method demonstrated proof-of-concept detection of clinically relevant concentration (2.5–25 copies/μL and 4.1–41 aM) of SARS-CoV-2 *RdRp* gene-bearing plasmid DNA and RNA from these samples. This work is novel in proving the superiority of indirect magneto-preconcentration (followed by in situ LAMP) over direct magneto-preconcentration in nucleic acid NAAT biosensing. It would be the first to do so with LAMP as the downstream in situ NAAT. This study is also probably the first to evaluate the role of hgDNA and serum-based polymerase inhibitors on sequence-specific direct and indirect magneto-extraction and downstream NAAT. In addition, the developed assay would be the first to demonstrate its effectiveness in magneto-extracting and detecting SARS-CoV-2 nucleic acid involving electrochemical readout. The study is general in nature and could be extended to detect non-SARS-CoV-2 pathogens. Similarly, the indirect magnetic enrichment could also be integrated with other NAATs. Overall, our assay provided a sensitive, low-cost, near-point-of-care, sample-to-answer, and non-instrument-intensive method for detecting pathogen nucleic acid.

Author statement

S.T., T.A., A.T., M.S., A.K., and S.G. envisioned the study. S.T. and S.G. designed, conducted, and analyzed the nucleic acid magnetocapture, in vitro transcription, and NAAT experiments. T.A. and A.K. designed, conducted, and analyzed the electrochemical measurements. M.S. guided plasmid procurement, microbiology, cell culture, and in vitro transcription. A.T. guided clinical perspectives of molecular diagnosis and requirements in limited-resource settings. S.T., T.A., M.S., A.K., and S.G. wrote the paper. All authors edited and approved the final manuscript.

Declaration of competing interest

The authors declare the following financial interests/personal relationships which may be considered as potential competing interests: Dr. Souradyuti Ghosh reports financial support was provided by Mission on Nano Science and Technology - Department of Science and Technology-Government of India for Nanomission grant. Dr. Souradyuti Ghosh reports financial support was provided by Department of Biotechnology, India grant. Dr. Souradyuti Ghosh has patent #202111028722 pending to Bennett University, India. Dr. Souradyuti Ghosh has patent #202111037358 pending to Bennett University.

Data availability

Data will be made available on request.

Acknowledgment

The authors are thankful to Mission on Nano Science and Technology, Department of Science and Technology, Government of India for Nanomission grant (ref no DST/NM/NB/2018/189) and Department of Biotechnology grant (ref no BT/PR40297/COD/139/6/2020). They are also thankful to the Bennett University seed grant awarded to Dr. Ashvani Kumar, and Bennett University Ph.D. scholarship for Mr. Sayantan Tripathy and Ms. Tanvi Agarkar. The authors are thankful to lab managers Mr Jitendra Khare and Mr Ved Prakash Gangwar for their assistance in day-to-day lab management. The authors also thank Mr. Vimal Kumar Devrani, Mr. Divyanshu Jaju, and Mr. Sohamveer for significant help in the financial management of the external grants. The authors are grateful to Prof. Rajinder S. Chauhan for constant scholarly support. Finally, the authors thank the reviewers and editors for the critical comments that helped improve the manuscript.

Appendix A. Supplementary data

Supplementary data to this article can be found online at https://doi.org/10.1016/j.talanta.2022.123809.

References

[1] Johns Hopkins Coronavirus Resource Center: Home, Johns Hopkins Coronavirus Resour. Cent. (n.d.). https://coronavirus.jhu.edu/(accessed January 24, 2022).
[2] Q. Diagnostics, FDA instructions on detectimg SARS-CoV-2 RNA with real-time RT-PCR, (n.d.). https://www.fda.gov/media/136231/download.
[3] M.J. Wacker, M.P. Godard, Analysis of one-step and two-step real-time RT-PCR using SuperScript III, J. Biomol. Tech. JBT. 16 (2005) 266–271.
[4] RT-PCR: One step vs. two step | IDT, Integr. DNA Technol. (n.d.). https://sg.idtdna.com/pages/support/faqs/what-are-the-advantages-and-disadvantages-of-one-step-vs.-two-step-rt-pcr (accessed December 4, 2021).
[5] V.L. Dao Thi, K. Herbst, K. Boerner, M. Meurer, L.P. Kremer, D. Kirrmaier, A. Freistaedter, D. Papagiannidis, C. Galmozzi, M.L. Stanifer, S. Boulant, S. Klein, P. Chlanda, D. Khalid, I. Barreto Miranda, P. Schnitzler, H.-G. Kräusslich, M. Knop, S. Anders, A colorimetric RT-LAMP assay and LAMP-sequencing for detecting SARS-CoV-2 RNA in clinical samples, Sci. Transl. Med. 12 (2020), eabc7075, https://doi.org/10.1126/scitranslmed.abc7075.
[6] J.P. Broughton, X. Deng, G. Yu, C.L. Fasching, V. Servellita, J. Singh, X. Miao, J. A. Streithorst, A. Granados, A. Sotomayor-Gonzalez, K. Zorn, A. Gopez, E. Hsu, W. Gu, S. Miller, C.-Y. Pan, H. Guevara, D.A. Wadford, J.S. Chen, C.Y. Chiu, CRISPR-Cas12-based detection of SARS-CoV-2, Nat. Biotechnol. 38 (2020) 870–874, https://doi.org/10.1038/s41587-020-0513-4.
[7] L. Yu, S. Wu, X. Hao, X. Dong, L. Mao, V. Pelechano, W.-H. Chen, X. Yin, Rapid Detection of COVID-19 Coronavirus Using a Reverse Transcriptional Loop-Mediated Isothermal Amplification (RT-LAMP) Diagnostic Platform, Clin. Chem. (n.d.). https://doi.org/10.1093/clinchem/hvaa102..
[8] N.Y. Jayanath, L.T. Nguyen, T.T. Vu, L.D. Tran, Development of a portable electrochemical loop mediated isothermal amplification (LAMP) device for detection of hepatitis B virus, RSC Adv. 8 (2018) 34954–34959, https://doi.org/10.1039/C8RA07235C.
[9] A. Anurup, A. Mostafa, J. Berger, M.Y. Aydin, F. Sun, S.A.S. de Ramirez, E. Valera, B.T. Cunningham, W.P. King, R. Bashir, Rapid isothermal amplification and portable detection system for SARS-CoV-2, Proc Natl Acad Sci U A 117 (2020) 22727–22735.
[10] J.D. Pearson, D. Trcka, S. Lu, S.J. Hyduk, M. Jen, M.-M. Aynaud, J.J. Hernández, P. Peidis, M. Barrios-Rodiles, K. Chan, J. Woodgett, T. Mazzulli, L. Attisano, L. Pelletier, M.I. Cybulsky, J.L. Wrana, R. Bremner, Comparison of SARS-CoV-2 indirect and direct RT-qPCR detection methods, Virol. J. 18 (2021) 99, https://doi.org/10.1186/s12985-021-01574-4.
[11] K. Taki, I. Yokota, T. Fukumoto, S. Iwasaki, S. Fujisawa, M. Takahashi, S. Negishi, K. Hayasaka, K. Sato, S. Oguri, M. Nishida, J. Sugita, S. Konno, T. Saito, T. Teshima, SARS-CoV-2 detection by fluorescence loop-mediated isothermal amplification with and without RNA extraction, J. Infect. Chemother. 27 (2021) 410–412, https://doi.org/10.1016/j.jiac.2020.10.029.
[12] L. Mautner, C.-K. Baillie, H.M. Herold, W. Volkwein, P. Guertler, U. Eberle, N. Ackermann, A. Sing, M. Pavlovic, O. Goerlich, U. Busch, L. Wassill, I. Huber, A. Baiker, Rapid point-of-care detection of SARS-CoV-2 using reverse transcription loop-mediated isothermal amplification (RT-LAMP), Virol. J. 17 (2020) 160, https://doi.org/10.1186/s12985-020-01435-6.
[13] M.N. Anahtar, G.E.G. McGrath, B.A. Rabe, N.A. Tanner, B.A. White, J.K. M. Lennerz, J.A. Branda, C.L. Cepko, E.S. Rosenberg, Clinical assessment and validation of a rapid and sensitive SARS-CoV-2 test using reverse transcription loop-mediated isothermal amplification without the need for RNA extraction, Open Forum Infect. Dis. 8 (2021), https://doi.org/10.1093/ofid/ofaa631 ofaa631.
[14] P. Oberacker, P. Stepper, D.M. Bond, S. Höhn, J. Focken, V. Meyer, L. Schelle, V. J. Sugrue, G.-J. Jeunen, T. Moser, S.R. Hore, F. von Meyenn, K. Hipp, T.A. Hore, T. P. Jurkowski, Bio-On-Magnetic-Beads (BOMB): open platform for high-throughput nucleic acid extraction and manipulation, PLoS Biol. 17 (2019), e3000107, https://doi.org/10.1371/journal.pbio.3000107.
[15] S. Tripathy, A.K. Chalana, A. Talukdar, P.V. Rajesh, A. Saha, G. Pramanik, S. Ghosh, Limited-resource preparable chitosan magnetic particles for extracting amplification-ready nucleic acid from complex biofluids, Analyst 147 (2021) 165–177, https://doi.org/10.1039/d1an01150b.
[16] C.-H. Wang, K.-Y. Lien, T.-Y. Wang, T.-Y. Chen, G.-B. Lee, An integrated microfluidic loop-mediated-isothermal-amplification system for rapid sample pretreatment and detection of viruses, Biosens. Bioelectron. 26 (2011) 2045–2052, https://doi.org/10.1016/j.bios.2010.08.083.
[17] S.P. Tsai, A. Wong, E. Mai, P. Chan, G. Mausisa, M. Vasser, P. Jhurani, M. H. Jakobsen, W.L.T. Wong, J.-P. Stephan, Nucleic acid capture assay, a new method for direct quantitation of nucleic acids, Nucleic Acids Res. 31 (2003) e25.
[18] C.-H. Wang, K.-Y. Lien, J.-J. Wu, G.-B. Lee, A magnetic bead-based assay for the rapid detection of methicillin-resistant Staphylococcus aureus by using a microfluidic system with integrated loop-mediated isothermal amplification, Lab Chip 11 (2011) 1521–1531, https://doi.org/10.1039/c0lc00430h.

[19] C.-L. Lin, W.-H. Chang, C.-H. Wang, C.-H. Lee, T.-Y. Chen, F.-J. Jan, G.-B. Lee, A microfluidic system integrated with buried optical fibers for detection of Phalaenopsis orchid pathogens, Biosens. Bioelectron. 63 (2015) 572–579, https://doi.org/10.1016/j.bios.2014.08.013.
[20] J. Chen, X. Xu, Z. Huang, Y. Luo, L. Tang, J.-H. Jiang, BEAMing LAMP: single-molecule capture and on-bead isothermal amplification for digital detection of hepatitis C virus in plasma, Chem. Commun. Camb. Engl. 54 (2018) 291–294, https://doi.org/10.1039/c7cc08403j.
[21] M.F. Österdahl, K.A. Lee, M.N. Lochlainn, S. Wilson, S. Douthwaite, R. Horsfall, A. Sheedy, S.D. Goldenberg, C.J. Stanley, T.D. Spector, C.J. Steves, Detecting SARS-CoV-2 at point of care: preliminary data comparing loop-mediated isothermal amplification (LAMP) to polymerase chain reaction (PCR), BMC Infect. Dis. 20 (2020) 783, https://doi.org/10.1186/s12879-020-05484-8.
[22] X. Hu, Q. Deng, J. Li, J. Chen, Z. Wang, X. Zhang, Z. Fang, H. Li, Y. Zhao, P. Yu, W. Li, X. Wang, S. Li, L. Zhang, T. Hou, Development and clinical application of a rapid and sensitive loop-mediated isothermal amplification test for SARS-CoV-2 infection, mSphere 5 (2020), https://doi.org/10.1128/mSphere.00808-20.
[23] S. Klein, T.G. Müller, D. Khalid, V. Sonntag-Buck, A.-M. Heuser, B. Glass, M. Meurer, I. Morales, A. Schillak, A. Freistaedter, I. Ambiel, S.L. Winter, L. Zimmermann, T. Naumoska, F. Bubeck, D. Kirrmaier, S. Ullrich, I. Barreto Miranda, S. Anders, D. Grimm, P. Schnitzler, M. Knop, H.-G. Kräusslich, V.L. Dao Thi, K. Börner, P. Chlanda, SARS-CoV-2 RNA extraction using magnetic beads for rapid large-scale testing by RT-qPCR and RT-LAMP, Viruses 12 (2020), https://doi.org/10.3390/v12080863.
[24] A.D. Yu, K. Galatsis, J. Zheng, J.Q. Le, D. Ma, S. Perlman, M. Rosbash, Development of a saliva-optimized RT-LAMP assay for SARS-CoV-2, J. Biomol. Tech. JBT. 32 (2021) 102–113, https://doi.org/10.7171/jbt.21-3203-005.
[25] A. Bektaş, M.F. Covington, G. Aidelberg, A. Arce, T. Matute, I. Núñez, J. Walsh, D. Boutboul, C. Delaugerre, A.B. Lindner, F. Federici, A.D. Jayaprakash, Accessible LAMP-enabled rapid test (ALERT) for detecting SARS-CoV-2, Viruses 13 (2021), https://doi.org/10.3390/v13050742.
[26] L.M. Dignan, M.S. Woolf, C.J. Tomley, A.Q. Nauman, J.P. Landers, Multiplexed centrifugal microfluidic system for dynamic solid-phase purification of polynucleic acids direct from buccal swabs, Anal. Chem. 93 (2021) 7300–7309, https://doi.org/10.1021/acs.analchem.1c00842.
[27] M. El-Tholoth, H.H. Bau, J. Song, A single and two-stage, closed-tube, molecular test for the 2019 novel coronavirus (COVID-19) at home, clinic, and points of entry, ChemRxiv Prepr. Serv. Chem. (2020), https://doi.org/10.26434/chemrxiv.11860137.
[28] K. Nawattanapaiboon, E. Pasomsub, P. Prombun, A. Wongbunmak, A. Jenjitwanich, P. Mahasupachai, P. Vetcho, C. Chayrach, N. Manatjaroenlap, C. Samphaongern, T. Watthanachockchai, P. Leedorkmai, S. Manopwisedjaroen, R. Akkarawongsapat, A. Thitithanyanont, M. Phanchana, W. Panbangred, S. Chauvatcharin, T. Srikhirin, Colorimetric reverse transcription loop-mediated isothermal amplification (RT-LAMP) as a visual diagnostic platform for the detection of the emerging coronavirus SARS-CoV-2, Analyst 146 (2021) 471–477, https://doi.org/10.1039/d0an01775b.
[29] W.S. Jang, D.H. Lim, J. Yoon, A. Kim, M. Lim, J. Nam, R. Yanagihara, S.-W. Ryu, B. K. Jung, N.-H. Ryoo, C.S. Lim, Development of a multiplex loop-mediated isothermal amplification (LAMP) assay for on-site diagnosis of SARS CoV-2, PLoS One 16 (2021), e0248042, https://doi.org/10.1371/journal.pone.0248042.
[30] X. Xie, K.G. Lokugamage, X. Zhang, M.N. Vu, A.E. Muruato, V.D. Menachery, P.-Y. Shi, Engineering SARS-CoV-2 using a reverse genetic system, Nat. Protoc. 16 (2021) 1761–1784, https://doi.org/10.1038/s41596-021-00491-8.
[31] Department of Health and Human Services, NIH Guidelines for Research Involving Recombinant or Synthetic Nucleic Acid Molecules, (n.d.). https://osp.od.nih.gov/wp-content/uploads/NIH_Guidelines.pdf.
[32] P. Zhou, X.-L. Yang, X.-G. Wang, B. Hu, L. Zhang, W. Zhang, H.-R. Si, Y. Zhu, B. Li, C.-L. Huang, H.-D. Chen, J. Chen, Y. Luo, H. Guo, R.-D. Jiang, M.-Q. Liu, Y. Chen, X.-R. Shen, X. Wang, X.-S. Zheng, K. Zhao, Q.-J. Chen, F. Deng, L.-L. Liu, B. Yan, F.-X. Zhan, Y.-Y. Wang, G.-F. Xiao, Z.-L. Shi, A pneumonia outbreak associated with a new coronavirus of probable bat origin, Nature 579 (2020) 270–273, https://doi.org/10.1038/s41586-020-2012-7.
[33] S. Shiehzadegan, N. Alaghemand, M. Fox, V. Venketaraman, Analysis of the Delta variant B.1.617.2 COVID-19, Clin. Pract. 11 (2021) 778–784, https://doi.org/10.3390/clinpract11040093.
[34] S.S.A. Karim, Q.A. Karim, Omicron SARS-CoV-2 variant: a new chapter in the COVID-19 pandemic, Lancet Lond. Engl. 398 (2021) 2126–2128, https://doi.org/10.1016/S0140-6736(21)02758-6.
[35] T.R. Tong, Severe acute respiratory syndrome coronavirus (SARS-CoV), Perspect. Med. Virol. 16 (2006) 43–95, https://doi.org/10.1016/S0168-7069(06)16004-8.
[36] N. Ramadan, H. Shaib, Middle East respiratory syndrome coronavirus (MERS-CoV): a review, Germs 9 (2019) 35–42, https://doi.org/10.18683/germs.2019.1155.
[37] J.N. Zadeh, C.D. Steenberg, J.S. Bois, B.R. Wolfe, M.B. Pierce, A.R. Khan, R. M. Dirks, N.A. Pierce, NUPACK: analysis and design of nucleic acid systems, J. Comput. Chem. 32 (2011) 170–173, https://doi.org/10.1002/jcc.21596.
[38] S.O. Kelley, What are clinically relevant levels of cellular and biomolecular analytes? ACS Sens. 2 (2017) 193–197, https://doi.org/10.1021/acssensors.6b00691.
[39] H.M. Pezzi, D.J. Niles, J.L. Schehr, D.J. Beebe, J.M. Lang, Integration of magnetic bead-based cell selection into complex isolations, ACS Omega 3 (2018) 3908–3917, https://doi.org/10.1021/acsomega.7b01427.
[40] N.M. Adams, H. Bordelon, K.-K.A. Wang, L.E. Albert, D.W. Wright, F.R. Haselton, Comparison of three magnetic bead surface functionalities for RNA extraction and detection, ACS Appl. Mater. Interfaces 7 (2015) 6062–6069, https://doi.org/10.1021/am506374t.
[41] C. Schrader, A. Schielke, L. Ellerbroek, R. Johne, PCR inhibitors - occurrence, properties and removal, J. Appl. Microbiol. 113 (2012) 1014–1026, https://doi.org/10.1111/j.1365-2672.2012.05384.x.
[42] CDC, CDC-Preparation of viral transport media, (n.d.). https://www.cdc.gov/coronavirus/2019-ncov/downloads/Viral-Transport-Medium.pdf.
[43] WHO Viral transport media (VTM), (n.d.). https://www.who.int/ihr/publications/Annex8.pdf?ua=1.
[44] CDC Viral Transport Media, (n.d.). https://www.cdc.gov/coronavirus/2019-ncov/downloads/Viral-Transport-Medium.pdf.
[45] A. Martin, L. Bouffier, K.B. Grant, B. Limoges, D. Marchal, Real-time electrochemical LAMP: a rational comparative study of different DNA intercalating and non-intercalating redox probes, Analyst 141 (2016) 4196–4203, https://doi.org/10.1039/c6an00867d.
[46] S.O. Kelley, J.K. Barton, N.M. Jackson, M.G. Hill, Electrochemistry of methylene blue bound to a DNA-modified electrode, Bioconjugate Chem. 8 (1997) 31–37, https://doi.org/10.1021/bc960070o.
[47] BGI-A Trusted Total Lab Solution for COVID-19 Pandemic, (n.d.). https://www.bgi.com/us/bgi-covid-19-total-lab-solution/(accessed December 8, 2021).
[48] GeneXpert® prices, FIND. (n.d.). https://www.finddx.org/pricing/genexpert/(accessed December 8, 2021).